Role of phonon coupling in the broadening of rotational lines of diatomics trapped in rare gas matrices. A model calculation for HCl in Ar

M. Allavena, H. Chakroun, and David White

Citation: J. Chem. Phys. **77**, 1757 (1982); doi: 10.1063/1.444071
View online: http://dx.doi.org/10.1063/1.444071
View Table of Contents: http://jcp.aip.org/resource/1/JCPSA6/v77/i4
Published by the American Institute of Physics.

Role of phonon coupling in the broadening of rotational lines of diatomics trapped in rare gas matrices. A model calculation for HCl in Ar

M. Allavena and H. Chakroun

Centre de Mécanique Ondulatoire Appliquée, 23, Rue du Maroc, 75940 Paris Cedex, France

David White[a)]

Laboratory for Research on the Structure of Matter and Department of Chemistry, University of Pennsylvania, Philadelphia, Pennsylvania 19104
(Received 5 April 1982; accepted 6 May 1982)

The near infrared spectra of HCl trapped in pure and N_2-doped Ar matrices at low temperature are reported. In pure Ar, a hindered rotational spectrum is obtained and the $R(0)$ line exhibits a strong temperature dependence. The "Q" feature observed in the N_2-doped experiment is rather insensitive to temperature. The temperature dependence of the rotational line is interpreted on the basis of a rotational-phonon coupling model. The absorption coefficient is calculated within the framework of the linear response theory applied to the case of a diatomic molecule embedded in a linear chain of matrix atoms. The calculated full-width at half-maximum is in good agreement with the observed trend.

I. INTRODUCTION

The near infrared region of HCl isolated in solid rare gas matrices has been widely investigated[1–20] because its spectrum is typical of hindered rotation of small molecules in solids. The recorded rotational-vibrational spectra clearly exhibit the $R(0)$, $R(1)$ lines associated with monomeric species, as well as other features assigned to polymeric HCl or associated species like HCl–N_2 and HCl–O_2. Furthermore, the pure rotational $J=1 \leftarrow J=0$ transition has been observed in both Ar and Kr[16] matrices confirming the $R(0)$ assignment in rotation-vibration spectrum. Phonon activated and local modes have been recorded,[10] and it has also been shown by laser excited vibrational fluorescence[20] studies that the dominant process of vibrational relaxation might be through rotational levels.

Paralleling these experimental studies, the theoretical investigation of the nature of the interaction of HCl with its crystal environment has been developed. A model for hindered rotation in crystalline solids was originally proposed by Pauling[21] and extended by Devonshire[22] to a more realistic case which gave the shifts and splittings of the free rotor energy levels in an octahedral field. Later the rotational-translational coupling (RTC) model[23–27] was specifically adapted to the matrix case to predict spectral features and interpret matrix shifts. Mannheim *et al*,[28] using RTC have obtained rough estimates of the $R(0)$, and $R(1)$ linewidths of HCl in Ar, Kr, and Xe; these are (in cm^{-1}) 0.4, 0.3, 0.3, respectively, for $R(0)$ and 10, 9, 2, respectively, for $R(1)$. A good deal of attention has focused on the problem of vibrational relaxation. Direct transfer of energy to the solid matrix medium by multiphonon processes[29] has been extensively considered.[30] However, recent experiments[31] have pointed to the rotational levels as intermediate steps in the energy transfer process, but the temperature dependence of the vibrational relaxation still indicates a phonon participation resulting from a coupling between rotational levels and lattice modes.

In spite of this enormous effort devoted to the study of HCl in matrices, a careful analysis of rotational line shape as a function of temperature is still not available. It is the purpose of the present work to examine both experimentally and theoretically the temperature dependence of the $R(0)$ feature of the rotational-vibrational spectrum of HCl trapped in a solid Ar matrix. The rotational spectrum between 4.3 and 30.5 K has been recorded and the changes in the linewidths at half-maximum (FWHM) for two of the most significant features $R(0)$ and "Q" with temperature have been measured. This temperature dependent broadening is interpreted on the basis of a phonon-rotational relaxation process. The rotational-phonon coupling is obtained by performing an expansion in lattice displacements to second order, of the intermolecular potential which represents the interaction of an HCl molecule with its nearest neighbors. The absorption coefficient is then calculated in the framework of the linear response theory. In order to make the problem tractable, calculations have been performed using a model in which the diatomic impurity is coupled to a linear chain of atoms simulating the matrix lattice modes.

In Sec. II, the experiments and experimental results are reported. The model and theoretical framework for the analysis of the data are given in Sec. III, but some details of calculations are found in the Appendix. Finally, Sec. IV summarizes the numerical calculations and gives a comparison with experiment.

II. EXPERIMENTAL

A. Apparatus

A conventional liquid, helium or hydrogen, cryostat similar to that employed by Mann, Acquista, and White[32]

[a)]The work at the University of Pennsylvania was supported by the National Science Foundation, MRL program under Grant No. DMR-7923647.

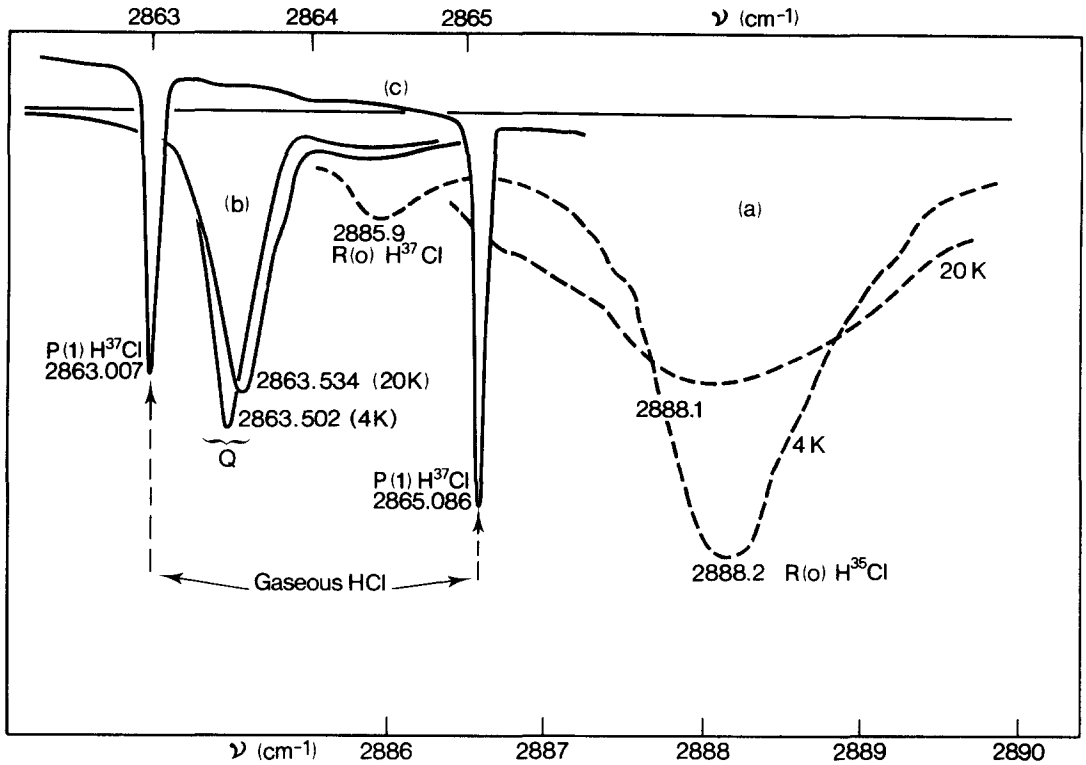

FIG. 1. Absorption spectra of HCl trapped in Ar matrix. (a) $R(0)$ line at 4 and 20 K (dotted line), (b) Q region at 4 and 20 K, (c) reference spectrum, gaseous HCl.

was used for the matrix isolation experiments in the vicinity of the boiling point of helium or hydrogen and the triple point of hydrogen. At higher temperatures the two stage open miniaturized Joule–Thompson (JT) liquifier described by White and Mann[33] was used. The latter has the advantage of permitting measurements over the entire range 15–35 K. In both cases, the matrix isolated HCl was deposited on an optically transparent sapphire window in thermal contact with either the liquid refrigerants or the cold end of the JT refrigeration system.

In all the experiments reported here, the matrix was deposited from a gaseous mixture containing one part of HCl, one part N_2, and 1200 parts pure argon on the sapphire window at 20 K at a rate of 100–200 μmol of mixture per minute. The N_2 was included to bring out the Q feature described in Ref. (32). This gas mixture was prepared in a thoroughly degassed high vacuum system and stored in a 1ℓ gas bulb overnight to ensure complete mixing. Since there is a tendency for HCl to be adsorbed on glass as well as metal surfaces, the glass storage bulbs as well as the stainless steel line leading to the cryostat were pickled overnight with a 1% HCl–Ar mixture before utilization.

The HCl used in these experiments was an isotopically enriched sample containing approximately 90% $H^{35}Cl$ obtained from the Stable Isotope Division, Oak Ridge National Laboratory. Its purity was greater than 99.99%. The purity of the argon obtained from the Matheson Corp. was better than 99.999%. Temperature measurements were made with a 1/2 W carbon resistance thermometer in good thermal contact with the O.F.H.C. copper mount supporting the sapphire cold window. The resistance thermometer was calibrated using both the vapor pressure of liquid parahydrogen and helium. The temperature of the argon matrix in the optical path is probably greater than that measured by the thermometer but by no more than a degree or so at worst.

The infrared spectra were taken with the high resolution spectrograph of the Laboratory of Molecular Spectroscopy at the Ohio State University which has already been described in detail by Rao and Fraley.[34]

Under the conditions of the present experiments, the best spectral resolution was approximately 0.04 cm^{-1}.

B. Results

The infrared spectrum in the vicinity of 2900 cm^{-1} of matrix isolated HCl at two different temperatures namely the boiling points of hydrogen and helium is illustrated in Fig. 1. The Ar matrix was formed at 20 K and cooled to 4 K. As we have demonstrated earlier,[32] such temperature cycling is completely reversible. The broken lines in Fig. 1 in the vicinity of 2888 cm^{-1} corresponds to the $R(0)$ feature of matrix isolated $H^{35}Cl$.[32] The 4 K spectrum unlike the broader 20 K shows a well resolved band due to the small amount of the $H^{37}Cl$ isotope present in the sample. The solid line at approximately 2863.5 cm^{-1} also depicts a band due to the matrix isolated HCl but the feature designated Q arises when impurities such as N_2 are introduced into the matrix.[33]

It is much narrower than the $R(0)$ band and the temperature dependence of the linewidth is much smaller. Also included in Fig. 1 is a superimposed spectrum of the $P(1)$ line of the ^{35}Cl and ^{37}Cl isotope of gaseous HCl at a pressure of a few Torr. It serves to illustrate the shifts as well as the broadening that occurs on matrix deposition.

In Table I, the temperature dependence of the band centers of both $R(0)$ and Q as well as the linewidth (FWHM) are summarized. The linewidth data are also shown in Fig. 2. These results compare favorably with the recent high resolution laser studies of Wiesenfeld and Moore[20] at 9 and 20 K.

Although the main purpose of the report is to account for the changes in linewidth with temperature of a matrix isolated HCl in a pure argon lattice in the ground rotational state $R(0)$ due to the phonon coupling, we have included the Q feature in the experimental investigation since it gives one a measure of the linewidth due to inhomogeneous broadening. Random lattice imperfections give rise to a distribution of HCl local environments. Fortunately, however, the effect is small as is evident from the data in Fig. 2.

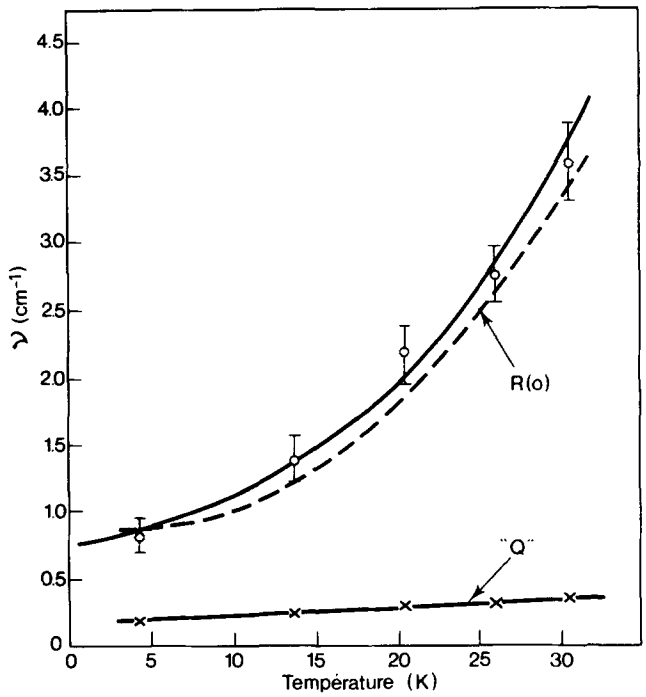

FIG. 2. Observed (continuous line) and calculated (dotted line) full width at half-maximum (FWHM) of the $R(0)$ line as a function of temperature. Observed FWHM of the Q branch is also represented at the bottom of the figure.

III. THEORY

A. General procedure

The calculation closely follows the method used to describe the spectral response of harmonic and anharmonic oscillators coupled to a phonon bath.[35,36] The linear response theory in the semiclassical approximation is adopted. In this context, the absorption coefficient of a sample containing infrared active molecules is given by

$$Q(\omega)=\frac{4\pi}{\hbar}\omega\,|f_0|^2\sum_{\mu,\nu}e_\mu e_\nu\,\mathrm{Im}\,G_{\mu\nu}(\omega)\,, \tag{1}$$

where ω, f_0, and $\mathbf{e}(e_\mu,\ \mu=x,y,z)$ are the frequency, amplitude, and polarization vector of the incoming infrared radiation. $\mathrm{Im}\,G_{\mu\nu}(\omega)$ is the imaginary part of the Fourier transform of the Green function

$$G(t-t')=-i\theta(t-t')\ \langle[\mathbf{M}(t)\cdot\mathbf{e},\mathbf{M}(t')\cdot\mathbf{e}]\rangle$$

$$=-i\theta(t-t')\sum_{\mu,\nu}e_\mu e_\nu\,\langle[M_\mu(t),M_\nu(t')]\rangle\,. \tag{2}$$

Here, $M(t)$ is the Heisenberg representation of the total dipole moment associated with the absorbing sample,

TABLE I. Experimentally observed variation of line position and linewidth (FWHM) with temperature for HCl in solid argon.

	$R(0)$		$"Q"$	
Temp. (K)	ν (cm^{-1})	$\Delta\nu$ (cm^{-1})	ν (cm^{-1})	$\Delta\nu$ (cm^{-1})
4.3	2888.2±0.1	0.85±0.1	2863.51±0.01	0.18±0.02
13.9	2888.2±0.1	1.4±0.2	2863.56±0.01	0.25±0.02
20.4	2888.1±0.1	2.2±0.2	2863.59±0.01	0.31±0.02
26.0	2888.0±0.2	2.8±0.3	2863.69±0.01	0.33±0.02
30.5	2888.0±0.2	3.6±0.3	2863.80±0.01	0.37±0.02

$\theta(t-t')$ is the step function, and the average ($\langle\cdots\rangle$) over the commutator ($[\cdots]$) is a canonical average defined, for any operator A, by

$$\langle A\rangle=(1/Z)\,Sp\cdot Ae^{-\beta H},\quad\text{with }\beta=1/kT\,, \tag{3}$$

k the Boltzmann constant, T the absolute temperature, Z the partition function, $Z=Sp\cdot e^{-\beta H}$, and H the time-independent Hamiltonian operator.

The core of the problem lies in the calculation of the Fourier transform $G_{\mu\nu}(\omega)\equiv\langle\langle M_\mu,M_\nu\rangle\rangle_\omega$. This can be achieved by solving either one equation or a set of coupled relations generated from a master equation[37]

$$\hbar\omega\,\langle\langle[M_\mu,H]^{(n)},M_\nu\rangle\rangle_\omega=\frac{\hbar}{2\pi}\langle[[M_\mu,H]^{(n)},M_\nu]\rangle$$

$$+\langle\langle[M_\mu,H]^{(n+1)},M_\nu\rangle\rangle\,. \tag{4}$$

When $n=0$, $[M_\mu,H]^{(0)}=M_\mu$ and a single equation is obtained. It immediately follows that for $n=1$, $[M_\mu,H]^{(1)}=[M_\mu,H]$, and $n=2$, $[M_\mu,H]^{(2)}=[[M_\mu,H],H]$ leading to 2 and 3 equations, respectively; a process that continues indefinitely. It is however stopped by decoupling the equation at some selected stage as discussed in Sec. IIID.

B. Model

The model consist of a diatomic nonrigid rotor AB (HCl impurity) coupled to an unperturbed phonon bath (Argon matrix), the latter being represented by a linear chain of atoms (m,f are the mass of the Ar atom and the nearest neighbor force constant, respectively). Details

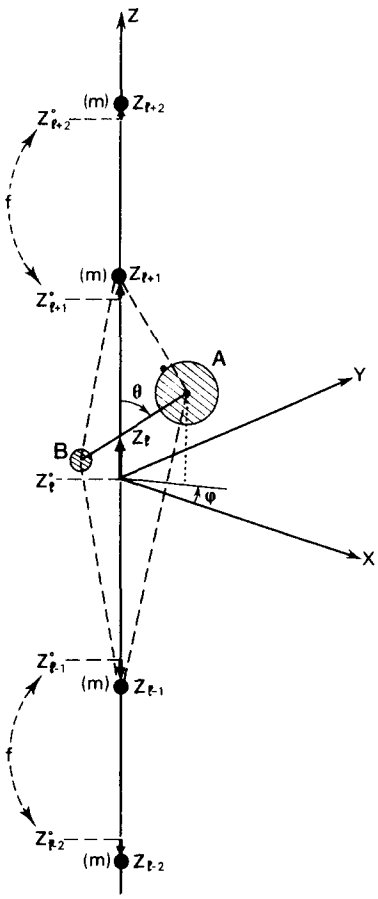

FIG. 3. A schematic representation of the model. z_l^0 and z_l are the equilibrium and instantaneous positions of the Ar atoms of mass m, respectively, f is the force constant between two Ar atoms.

of geometrical arrangement are depicted on Fig. 3. It is assumed that the concentration of the impurity molecules in the matrix is sufficiently low that interactions between impurities can be neglected. The center of mass of the molecular impurity occupies a site on the linear chain coordinate z_l and is constrained to remain on the chain axis. This simplified version of the physical situation requires the coincidence of both center of mass and center of interaction of the impurity molecule. Separability of vibrational and rotational motions is assumed and allows one to consider independently the coupling of each motion with the lattice. The vibrational shift, which may be evaluated from the v dependence (v: vibrational quantum number) of the intermolecular potential, [23] is not examined here. It may be taken into account by replacing the unperturbed vibrational frequency of the nonrigid rotor by an effective frequency, including such a frequency shift. As for the direct coupling of rotation with lattice modes it is realized by assuming that atoms A and B of the molecular impurity are bonded to the lattice nearest neighbors atoms (atom $l+1$ and $l-1$ of Fig. 3) by forces described by a potential $V(R, \mathbf{z}, \theta)$. R is the internuclear distance in the molecule, $\mathbf{z}$ is a vector the components of which are z_{l-1}, z_l, and z_{l+1}, θ is the angle between both molecular and chain axis. An analytical expression of V could be derived by using atom–atomlike potential such as the 6-12 Lennard-Jones (LJ) interatomic potentials. But no attempt has been made in this direction since it would lead to cumbersome calculations, which do not match the oversimplified version of the linear model. Furthermore, even in the framework of a more realistic approach, the semiempirical intermolecular potential available depends on poorly known coefficients (ϵ, σ in the case of LJ). Therefore, it has been preferred to deduce a simple form of the potential consistent with symmetry constraints and reasonable physical assumptions. The cylindrical symmetry imposed by our model requires that the potential function V is periodic in θ and can be expanded as a cosine Fourier series

$$V(R, \mathbf{z}, \theta) = \sum_{n=0}^{\infty} V^{(n)}(R, \mathbf{z}) \cos n\theta \ , \tag{5}$$

where $V(-\theta) = V(\theta)$. When the Ar atoms occupy their equilibrium position $z^0_{l-1} - z^0_l = a$, the constant defining the lattice parameter.

$$V(R^0, \mathbf{z}^0, \theta) = V(R^0, \mathbf{z}^0, \pi - \theta) \tag{6}$$

and symmetry considerations require that n be an even integer. However, when Ar atoms are displaced from these positions, condition (6) no longer applies and both odd and even terms of the expansion must be retained. Furthermore, the coefficients $V^{(n)}(R, \mathbf{z})$ can also be expanded in Taylor series in terms of the displacements of R and $\mathbf{z}$ with respect to their equilibrium position R^0 and $\mathbf{z}^0$. Both Taylor and Fourier expansions represent infinite series which have to be truncated, in order that the problem be tractable. In deciding the number of terms retained, we were guided by the following considerations: (a) Fourier series. Here the summation has been terminated at $n = 2$,

$$V = V^{(0)} + V^{(1)} \cos\theta + V^{(2)} \cos 2\theta \ .$$

These three terms still preserve, in the equilibrium lattice ($V^{(1)} = 0$), the characteristic feature of the linear model; i.e., a pseudoequilibrium position for the HCl molecule at $\theta^0_k = (2k+1)\pi/2$, $k = 0, 1, 2\ldots$ provided $V^{(0)}$ is negative and $V^{(2)}$ positive. When $V^{(1)}$ is different from zero, symmetry with respect to the θ^0_k axes is lost. This distortion of the crystal environment tends to shift the potential minima on one or the other side of the θ^0_k axis. Addition of higher terms ($n > 2$) would neither change drastically these features nor bring more physical insight to the model. (b) Taylor series. The expansion is performed to second order about an equilibrium position which can be defined with respect to the angularly averaged potential $V^{(0)}$ by the relations

$$\left(\frac{\partial V^{(0)}}{\partial R}\right)_e = 0 \ , \quad \left(\frac{\partial V^{(0)}}{\partial \mathbf{z}}\right)_e = 0 \ . \tag{7}$$

The internuclear distance R_e for the impurity molecule and new lattice parameter $\mathbf{z}_e$ for the linear chain determined from Eq. (7) are in general different from the equilibrium values R^0 and $\mathbf{z}^0$ associated with the separated systems. Thus,

$$V^{(n)}(R, \mathbf{z}) = V^{(n)}(R_e \mathbf{z}_e) + \left(\frac{\partial V^{(n)}}{\partial R}\right)_e R + \left(\frac{\partial V^{(n)}}{\partial \mathbf{z}}\right)_e \mathbf{z} + \tfrac{1}{2} R \left(\frac{\partial^2 V^{(n)}}{\partial R^2}\right)_e R + R \left(\frac{\partial^2 V^{(n)}}{\partial R \partial \mathbf{z}}\right)_e \mathbf{z} + \tfrac{1}{2} \mathbf{z} \left(\frac{\partial^2 V^{(n)}}{\partial \mathbf{z} \partial \mathbf{z}'}\right)_e \mathbf{z}' , \quad (8)$$

$n = 0, 1, 2$.

From Eq. (7) it follows that the linear terms in R and z are identically zero for $n = 0$, but not in the other two cases ($n = 1, 2$). To simplify the calculation it has been assumed that R_e, $\mathbf{z}_e$ do not differ appreciably from R^0 and $\mathbf{z}^0$. This is consistent with our model of an unperturbed phonon bath i.e., the perfect lattice approximation, where the lattice modes are unaffected by the presence of the impurity, which is in fact the basis for neglecting all second order terms in $\mathbf{z}\mathbf{z}'$. The constant term $V^{(1)}$ is, from symmetry considerations, equal to zero. As for $R\mathbf{z}$, it represents the coupling of pure vibration with phonon modes and previous calculations,[35] as well as simple energetic considerations, suggest that these terms must have a very small effect on shifting or broadening of the lines. This is true for both the $Rz \cos\theta$ and $R^n \cos n\theta$ ($n = 1, 2$) terms if we admit that trapping does not enhance the vibrational-rotational coupling. The interaction potential [Eq. (8)] is thus simply the sum of zero, one, and two phonons contributions,

$$V(R, \mathbf{z}, \theta) = V^{(0)}(R^0, \mathbf{z}^0) + \tfrac{1}{2} R \left(\frac{\partial^2 V^{(0)}}{\partial R^2}\right)_0 R + V^{(2)}(R^0 \mathbf{z}^0) \cos 2\theta + \left(\frac{\partial V^{(1)}}{\partial \mathbf{z}}\right)_0 \mathbf{z} \cos\theta + \left(\frac{\partial V^{(2)}}{\partial \mathbf{z}}\right)_0 \mathbf{z} \cos 2\theta + \tfrac{1}{2} \mathbf{z} \left(\frac{\partial^2 V^{(1)}}{\partial \mathbf{z} \partial \mathbf{z}'}\right)_0 \mathbf{z}' \cos\theta + \tfrac{1}{2} \mathbf{z} \left(\frac{\partial^2 V^{(2)}}{\partial \mathbf{z} \partial \mathbf{z}'}\right)_0 \mathbf{z}' \cos 2\theta . \quad (9)$$

Taking into account symmetry requirements and considering only nearest neighbor interactions transforms V into the following expression:

$$V(R, \mathbf{z}, \theta) = V^{(0)} + \tfrac{1}{2} K' R^2 + V^{(2)} \cos 2\theta + \lambda_1 [(z_{l+1} - z_l) - (z_l - z_{l-1})] \cos\theta + \lambda_2 (z_{l+1} - z_{l-1}) \cos 2\theta + \tfrac{1}{2} \Lambda_1 [(z_{l+1} - z_l)^2 - (z_l - z_{l-1})^2] \cos\theta + \tfrac{1}{2} \Lambda_2 [(z_{l+1} - z_l)^2 + (z_l - z_{l-1})^2] \cos 2\theta , \quad (10)$$

with

$$K' = \left(\frac{\partial^2 V^{(0)}}{\partial R^2}\right)_0 \quad \lambda_1 = \left(\frac{\partial V^{(1)}}{\partial z_{l-1}}\right)_0 , \quad \lambda_2 = \left(\frac{\partial V^{(2)}}{\partial z_{l-1}}\right)_0 , \quad \Lambda_1 = \left(\frac{\partial^2 V^{(1)}}{\partial z_{l-1}^2}\right)_0 , \quad \Lambda_2 = \left(\frac{\partial^2 V^{(2)}}{\partial z_{l-1}^2}\right)_0 . \quad (11)$$

The physical significance of each of these constant is as follows: $V^{(0)}$, as already stated, is the averaged intermolecular potential V. Since K' results from the dependence of V on the molecular internal coordinate R, it increases the internal force constant of the trapped molecule leading to a small blue shift in the vibrational frequency. This is of no importance here since we are not concerned with vibrational shifts. The static potential (rotational barrier) resulting from the interaction of the molecule with nearest neighbor lattice atoms is represented by $V^{(2)}$. Dynamical contributions are represented by the forces λ_1, λ_2 which displace the molecule along with the lattice atoms motion; Λ_1 and Λ_2 are the corresponding force constants. With the above potential it is now possible to write the complete Hamiltonian associated with a diatomic molecule embedded in a linear chain of rare gas atoms, in the form

$$H = H_0(R, \theta, \phi) + H_L(z_l) + V(R, \theta, \mathbf{z}) , \quad (12)$$

where H_0 and H_L are the unperturbed molecular and lattice Hamiltonians. In this expression, the kinetic perturbation term which introduces pure phonon terms weighted by the factor $1 - m/M$ (M mass of the molecule) is neglected since m and M of the HCl/Ar pair are very close. It also may be considered a consequence of the perfect lattice approximation.

Finally, for the dipole moment operator, which is traditionally written as an expansion with respect to R and z_l, only the term corresponding to vibrational-rotational transition

$$\mathbf{M} = \left(\frac{\partial |\mathbf{M}|}{\partial R}\right)_0 R \mathbf{m}_D , \quad (13)$$

where $\mathbf{m}_D$ is a unitary vector directed along the molecular axis, has been kept.

C. Representation

A projector formalism is adopted to represent the Hamiltonian and dipolar operators since the usual raising and lowering operators are not appropriate for more than two level systems. The unperturbed molecular Hamiltonian is projected onto the $|v\rangle|lm\rangle$ states. (v, l, m are the vibrational and rotational quantum numbers.) Defining $|v\rangle = C_v^+$ and $\langle v| = C_v$ and $|lm\rangle = D_{lm}^+$, $\langle lm| = D_{lm}$ one obtains

$$H_0 = \hbar\omega_M \sum_{v=0}^{\infty} (v + \tfrac{1}{2}) C_v^+ C_v + \sum_{lm} \epsilon_l D_{lm}^+ D_{lm} . \quad (14)$$

Note that

$$C_v C_{v'}^+ = \delta_{vv'} , \quad \sum_v C_v^+ C_v = 1 ,$$

$$D_{lm} D_{l'm'}^+ = \delta_{ll'} \delta_{mm'} , \quad \sum_{lm} D_{lm}^+ D_{lm} = 1 , \quad (15)$$

$\omega_M = (2\pi)^{-1} (K/\mu)^{1/2}$, $\epsilon_l = Bl(l+1)$, where K, μ, and B are the force constant, reduced mass, and rotational constant, respectively, of the molecular impurity. K can be considered as an effective force constant which takes into account the cage effect in order to reproduce vibrational shift (see Sec. III B). The phonon bath is represented with the help of the traditional set of creation operators b_k, b_{-k}^+ which are related to the instantaneous z_l coordinates of the rare gas atoms in the chain by

$$z_l = (\hbar/mN)^{1/2} \sum_k (2\omega_k)^{1/2} (b_k + b_{-k}^+) \exp ikz_l^0 , \quad (16)$$

N is the number of atoms in the chain, $k = |\mathbf{k}|$, $\mathbf{k}$ is the wave vector, ω_k the normal mode frequency, and z_l^0 is the equilibrium position of the lth atom. For reasons of convenience, the following dimensionless operators:

$$\phi_k = (2)^{-1/2}(b^+_{-k} + b_k)\ , \quad \pi_k = (2)^{-1/2}(b^+_k - b_{-k}) \tag{17}$$

are used in the calculation, which gives a lattice Hamiltonian

$$H_L = 2^{-1}\sum_k \hbar\omega_k(\phi_k\,\phi_{-k} - \pi_k\,\pi_{-k})\ , \tag{18}$$

with commutation rules

$$[\phi_k, \pi_{k'}] = \delta_{kk'}\ , \quad [\phi_k, C^+_v] = 0\ , \quad [\phi_k, D^+_{lm}] = 0, \ldots\ . \tag{19}$$

Using this set of operators, the interaction potential is easily transformed into operator form, and the complete Hamiltonian is

$$H = \hbar\bar{\omega}_M \sum_{v=0}^{\infty}(v+\tfrac{1}{2})\,C^+_v C_v + \sum_{lm}\bar{\epsilon}_{lm} D^+_{lm} D_{lm} + (2)^{-1}\sum_k \hbar\omega_k(\phi_k\phi_{-k} - \pi_k\pi_{-k}) + V^{(2)}\sum_{lm} A_2(l,m)\,(D^+_{l+2,m} D_{lm} + D^+_{lm} D_{l+2,m})$$
$$+ \sum_{n=1}^{2}\left\{\sum_{lmk}[\lambda_n\alpha_n(k)\phi_k + \Lambda_n\beta_n(k,k')\phi_k\phi_{k'}]\,[A_n(l,m)(D^+_{l+n,m}D_{lm} + D^+_{lm}D_{l+n,m}] + \delta(2-n)A_3(l,m)\,D^+_{lm}D_{lm}\right\}\ , \tag{20}$$

$\delta(2-n)$ is the Kronecker symbol and $\bar{\omega}_M$, $\bar{\epsilon}_m$ are the vibrational and rotational energies corrected for zero phonon level shifts

$$\bar{\omega}_M = (2\pi)^{-1}\,[(K+K')/\mu]^{1/2}\ ,$$
$$\bar{\epsilon}_{lm} = \epsilon_l + V^{(2)}\,A_0(lm)\ . \tag{21}$$

Analytical expressions of the coefficients A_1, A_2, A_3, $\alpha_1(k)$, $\alpha_2(k)$, $\beta_1(k,k')$, and $\beta_2(k,k')$ are given in the Appendix. The dipole moment operator can be also expanded using the same operator basis set and since only the $\Delta l = 1$, $\Delta m = 0$ transition is considered, the operator can be restricted to the M_z component

$$M_z(t) = \left(\frac{\partial|\mathbf{M}|}{\partial R}\right)_0 \sum_{v,lm}[(v+1)/2\gamma]^{1/2}\,M^v_z(t)\,M^{lm}_z(t)$$
$$= \sum_{vlm} M_v\,M^v_z(t)\,M^{lm}_z(t)\ , \tag{22}$$

with

$$M_v = \left(\frac{\partial|\mathbf{M}|}{\partial R}\right)_0[(v+1)/2\gamma]^{1/2}\ ,$$

where $\gamma = \omega_M/\hbar$, and

$$M^v_z(t) = C^+_v(t)\,C_{v+1}(t) + C^+_{v+1}(t)\,C_v(t)\ ,$$
$$M^{lm}_z(t) = A_1(lm)[D^+_{lm}(t)\,D_{l+1m}(t) + D^+_{l+1m}(t)\,D_{lm}(t)]\ . \tag{23}$$

The time evolution of the unperturbed operator is

$$C_v(t) = |v\rangle\exp[-i\omega_M(v+1/2)t]\ , \tag{24}$$

with similar expressions for the other cases.

D. Propagator equation in Fourier space

Using the dipole moment operator given by Eq. (22), the function $\langle\langle M_z, M_z\rangle\rangle_\omega$ in the left-hand side of Eq. (4) (case $n=0$) becomes

$$\langle\langle M_z, M_z\rangle\rangle_\omega = \sum_{\substack{vlm\\ v'l'm'}} M_v M_{v'}\,\langle\langle M^v_z M^{lm}_z\,|\,M^{v'}_z M^{l'm'}_z\rangle\rangle_\omega\ . \tag{25}$$

Every term in this sum is associated with a transition characterized by $vlm - v'l'm'$. The relevant Green function for a particular transition is

$$G(l,l') = \langle\langle C^+_v C_{v+1} D^+_{lm} D_{l'm}\,|\,M^{v'}_z\,M^{l'm}_z\rangle\rangle_\omega\ , \tag{26}$$

which satisfies the equation

$$\hbar\omega G(l,l') = \hbar(2\pi)^{-1}\,\langle[C^+_v C_{v+1} D^+_{lm} D_{l'm},\ M^{v'}_z M^{l'm}_z]\rangle$$
$$+ \langle\langle[C^+_v C_{v+1} D^+_{lm} D_{l'm},\ H]\,|\,M^{v'}_z M^{l'm}_z\rangle\rangle \tag{27}$$

once the commutator containing the H operator is worked out, Eq. (27) becomes

$$[\hbar(\omega - \bar{\omega}_M) - (\bar{\epsilon}_{l'm} - \bar{\epsilon}_{lm})]\,G(l,l') = (\hbar/2\pi)[(n_v n_{lm} - n_{v+1}n_{l-1m})\,A_1(l-1,m)\,\delta_{l,l'+1} - (n_v n_{lm} - n_{v+1}n_{l+1m})\,A_1(lm)\,\delta_{l,l'}]$$
$$+ V^{(2)}S^{(-)}_0(G) + \lambda_2\sum_k \alpha_2(k)\,S^{(-)}_1(G_k) + \Lambda_2\sum_{kk'}\beta_2(k,k')S^{(-)}_1(G_{kk'}) + \lambda_1\sum_k\alpha_1(k)t^{(-)}(G_k) + \Lambda_1\sum_{kk'}\beta_1(kk')t^{(-)}(G_{kk'})\ , \tag{28}$$

where n_v and n_{lm} are occupation numbers. They can be calculated from the general formula

$$n = Sp\,\hat{n}e^{-\beta H}\ ,$$

with $\hat{n} = C^+_v C_v$ or $D^+_{lm}D_{lm}$ using the Hamiltonian Eqs. (12) and (20). In the present calculation, we have, for simplicity, used the unperturbed molecular and lattice occupation numbers. This approximation assumes that coupling between rotational motion and lattice modes is sufficiently weak so that the second order perturbation correction to n term may be neglected. The experimentally observed nearly free rotation of HCl in the matrix environment, supports this assumption. Furthermore,

$$S^{(\pm)}_i(G) \equiv S^{(\pm)}_i[G(ll')] = A_2(l',m)\,G(l,l'+2) \pm A_2(l-2,m)\,G(l-2,l')$$
$$+ A_2(l'-2,m)\,G(l,l'-2) \pm A_2(l,m)\,G(l+2,l') + \delta_{i1}[A_3(l',m) - A_3(l,m)]\,G(l,l')\ , \tag{29}$$

$\delta_{i1}(i=0,1)$ is the Kronecker symbol. When $i=1$, the $G(L,L')$, with $(L,L')=(l,l'+2)$, $(l-2,l')$, $(l,l'-2)$, and $(l+2,l')$ have to be replaced successively by the functions

$$G_k(L,L')=\langle\langle C_v^+C_{v+1}D_{Lm}^+D_{L'm}\phi_k \,|\, M_z^{v'}M_z^{L'm'}\rangle\rangle \tag{30}$$

and

$$G_{kk'}(L,L')=\langle\langle C_v^+C_{v+1}D_{Lm}^+D_{L'm}\phi_k\phi_{k'} \,|\, M_z^{v'}M_z^{L'm'}\rangle\rangle\ , \tag{31}$$

which are new higher Green functions generated from the second commutator in Eq. (27). Likewise,

$$t^{(\pm)}(G_k)=t^{(\pm)}[G_k(ll')]=A_1(l',m)\,G_k(l,l'+1)\pm A_1(l-1,m)\,G_k(l-1,l')+A_1(l'-1,m)\,G_k(l,l'-1)\pm A_1(l,m)\,G_k(l+1,l')\ . \tag{32}$$

By application of the random phase approximation (RPA),

$$G_{kk'}(L,L')\simeq\langle\phi_k\phi_{k'}\rangle\,G(L,L')=(n_k+1/2)\,\delta_{-k,k'}\,G(L,L')\ , \tag{33}$$

where n_k is the phonon occupation number ($\hat{n}=b_k^+b_k$). Then, Eq. (28) becomes

$$\{\hbar(\omega-\bar{\omega}_M)-(\bar{\epsilon}_{l'm}-\bar{\epsilon}_{lm})-\Lambda_2N(T)\,[A_3(l'm)-A_3(l,m)]\}G(l,l')=(\hbar/2\pi)\,[(n_vn_{lm}-n_{v+1}n_{l-1m})\,A_1(l-1,m)\,\delta_{l,l'+1}$$

$$-(n_vn_{lm}-n_{v+1}n_{l+1m})\,A_1(l,m)\,\delta_{l,l'-1}]+[V^{(2)}+\Lambda_2N(T)]\,S_0^{(-)}(G)+\lambda_2\sum_k\alpha_2(k)\,S_1^{(-)}(G_k)+\lambda_1\sum_k\alpha_1(k)t^{(-)}(G_k)\ , \tag{34}$$

with

$$N(T)=\sum_k\beta_2(k,-k)(n_k+1/2)\ . \tag{35}$$

The corresponding summation with $\beta_1(k,-k)$ vanishes because of symmetry. From Eq. (34) the $G(l,l')$ are related to the Green function $G_k(L,L')$, the equation of motion for the latter being

$$[\hbar(\omega-\bar{\omega}_M)-(\bar{\epsilon}_{L'm}-\bar{\epsilon}_{Lm})]\,G_k(L,L')=-\hbar\omega_k\,\Pi_{-k}(L,L')+V^{(2)}S_0^{(-)}(G_k)+\lambda_2\sum_{k'}\alpha_2(k')\,S_1^{(-)}(G_{kk'})$$

$$+\Lambda_2\sum_{k'k''}\beta_2(k'k'')S_1^{(-)}(G_{k'k''k})+\lambda_1\sum_{k'}\alpha_1(k')t^{(-)}(G_{kk'})+\Lambda_1\sum_{k'k''}\beta_1(k'k'')t^{(-)}G_{k'k''k})\ , \tag{36}$$

where the new Green functions

$$\Pi_{-k}(L,L')=\langle\langle C_v^+C_{v+1}D_{Lm}^+D_{L'm}\,\pi_{-k} \,|\, M_z^{v'}M_z^{L'm}\rangle\rangle \tag{37}$$

and

$$G_{k'k''k}(\mathcal{L},\mathcal{L}')=\langle\langle C_v^+C_{v+1}D_{\mathcal{L}m}^+D_{\mathcal{L}'m}\phi_{k'}\phi_{k''}\phi_k \,|\, M_z^{v'}M_z^{\mathcal{L}'m}\rangle\rangle \tag{38}$$

are now introduced. As in Eqs. (29) and (32), $(\mathcal{L},\mathcal{L}')$ may take the values $(L,L'\pm2)$, $(L\pm2,L')$ or $(L,L'\pm1)$, $(L\pm1,L')$. Following the same procedure as before, the equation of motion of $\Pi_{-k}(L,L')$ is immediately written as

$$[\hbar(\omega-\bar{\omega}_M)-(\bar{\epsilon}_{L'm}-\bar{\epsilon}_{Lm})]\Pi_{-k}(L,L')=-\hbar\omega_kG_k(L,L')+V^{(2)}S_0^{(-)}(\Pi_{-k})+\lambda_2\sum_{k'}\alpha_2(k')S_1^{(-)}(\Pi_{-k,k'})$$

$$+\Lambda_2\sum_{k'k''}\beta_2(k',k'')S_1^{(-)}(\Pi_{-kk'k''})+\lambda_1\sum_{k'}\alpha_1(k')t^{(-)}(\Pi_{-k,k'})+\Lambda_1\sum_{k'k''}\beta_1(k',k'')t^{(-)}(\Pi_{-kk'k''})\ . \tag{39}$$

However, Eq. (39) is not strictly equivalent to Eq. (36) due to the noncommutativity of the operators π_k and ϕ_k [Eq. (19)]. As a consequence in $S^{(1)}$ and $t^{(+)}$ the functions

$$\Pi_{-kk'}(\mathcal{L},\mathcal{L}')=\langle\langle C_v^+C_{v+1}D_{\mathcal{L}m}^+D_{\mathcal{L}'m}\Pi_{-k}\phi_{k'} \,|\, M_z^{v'}M_z^{\mathcal{L}'m}\rangle\rangle\ , \tag{40}$$

$$\Pi_{-kk'k''}(\mathcal{L},\mathcal{L}')=\langle\langle C_v^+C_{v+1}D_{\mathcal{L}m}^+D_{\mathcal{L}'m}\Pi_{-k}\phi_{k'}\phi_{k''} \,|\, M_z^{v'}M_z^{\mathcal{L}'m}\rangle\rangle \tag{41}$$

are preceded by positive sign, whereas their conjugate $\Pi_{k',-k}$ and $\Pi_{k'k'',-k}$ (where the exchange of indices implies also exchange of the corresponding operators) are preceded by minus sign. Using the RPA approximation, Eqs. (36) and (39) becomes

$$[\hbar(\omega-\bar{\omega}_M)-(\bar{\epsilon}_{L'm}-\bar{\epsilon}_{Lm})]G_k(L,L')=-\hbar\omega_k\,\Pi_{-k}(L,L')+V^{(2)}S_0^{(-)}(G_k)+\lambda_2\alpha_2(k)\,(n_k+1/2)S_1^{(-)}(G)$$

$$+\Lambda_2\left[N(T)+2(n_k+1/2)\sum_{k'}\beta_2(k',-k)\right]S_1^{(-)}(G_k)+\lambda_1\alpha_1(k)\,(n_k+1/2)t^{(-)}(G)+\Lambda_1(n_k+1/2)\sum_{k'}\beta_1(k',-k)t^{(-)}(G_k)\ ,$$

$$[\hbar(\omega-\bar{\omega}_M)-(\bar{\epsilon}_{L'm}-\bar{\epsilon}_{Lm})]\,\Pi_{-k}(L,L')=-\hbar\omega_kG_k(L,L')+V^{(2)}S_0^{(-)}(\Pi_{-k})-(1/2)\lambda_2\alpha_2(k)S_1^{(+)}(G)$$

$$+\Lambda_2N(T)S_1^{(-)}(\Pi_{-k})-\Lambda_2\sum_{k'}\beta_2(k,-k')S_1^{(+)}(G_k)-(1/2)\lambda_1\alpha_1(k)t^{(+)}(G)-\Lambda_1\sum_{k'}\beta_1(k,-k')t^{(+)}(G_k)\ . \tag{42}$$

The basic equations from which $G(l,l')$ can be deduced are constituted by Eq. (34) and the system (42). Assuming that the coupling constants λ_s and Λ_s ($s=1,2$) are small, terms above second order in λ_s or Λ_s can be neglected,

and since the G_k are first order terms in Eq. (34), only a first order solution to the system (42) are needed. Neglecting first order term in Eq. (42), this system becomes

$$\Omega_{L,L'}G_k(L,L') = -\hbar\omega_k\Pi_{-k}(L,L') + \lambda_2\alpha_2(k)(n_k+1/2)S_1^{(-)}(G) - \lambda_1\alpha_1(k)(n_k+1/2)t^{(-)}(G)\ ,$$
$$\Omega_{L,L'}\Pi_{-k}(L,L') = -\hbar\omega_k G_k(L,L') - (1/2)\lambda_2\alpha_2(k)S_1^{(+)}(G) - (1/2)\lambda_1\alpha_1(k)t^{(+)}(G)\ , \tag{43}$$

with

$$\Omega_{L,L'} = \hbar(\omega-\bar{\omega}_M) - (\bar{\epsilon}_{L'M}-\bar{\epsilon}_{Lm}) - \Lambda_2 N(T)\left[A_3(L',m) - A_3(L,m)\right]\ . \tag{44}$$

Elimination of $\Pi_{-k}(L,L')$ between the two Eqs. of (42) leads to

$$(\Omega_{L,L'}^2 - \hbar\omega_k^2)G_k(L,L') = \lambda_1\alpha_1(k)\left[(1/2)\hbar\omega_k t^{(+)}(G) - (n_k+1/2)\,\Omega_{L,L'}t^{(-)}(G)\right]$$
$$+\lambda_2\alpha_2(k)\left[(1/2)\hbar\omega_k S_1^{(+)}(G) - (n_k+1/2)\,\Omega_{LL'}S_1^{(-)}(G)\right]\ . \tag{45}$$

And finally, all $G(L,L')$ functions appearing in $t^{(\pm)}(G)$ and $S_1^{(\pm)}(G)$ in Eq. (45) are replaced by their zero order approximation [see Eq. (28)]

$$G(L,L') = \frac{\hbar}{2\pi}\,\frac{(n_v n_{L,m} - n_{v+1}n_{L-1,m})A(L-1,m)\delta_{L,L'+1} + (n_v n_{L,m} - n_{v+1}n_{L+1,m})A_1(L,m)\delta_{L,L'-1}}{\hbar(\omega-\bar{\omega}_M) - (\bar{\epsilon}_{L'm} - \bar{\epsilon}_{Lm})}\ .$$

The solutions $G_k(L,L')$ derived from Eq. (45) are substituted into Eq. (34) and the required solution $G(l,l')$ is found. For the transition considered here, i.e., $l=0$, $l'=1$, the relation for $G(0,1)$ is shown below [Eq. (46)]. Note that the temperature dependent coefficient in Eq. (46) are n_{00}, n_{10}, and n_k, the rotational and phonon occupation numbers, respectively, and $\Gamma \equiv \Gamma(T) = [V^{(2)} + \Lambda_2 N(T)]\hbar^{-1}$, where $V^{(2)}$, Λ_2 are defined by Eq. (10), and $N(T)$ by Eq. (35) (see also the Appendix). Since the $l=2$ level is almost depopulated in the temperature range under consideration, in the following formula, all terms multiplied by the rotational population number n_{20} have been neglected:

$$G(0,1)\left(\omega-\bar{\omega}_M - 20 - \frac{8}{15}\Gamma - \frac{4}{15}\Gamma^2\left[\frac{3}{35}\,\frac{1}{\omega-\bar{\omega}_M-120-(16/45)\Gamma} + \frac{1}{15}\,\frac{1}{\omega-\bar{\omega}_M+40-(16/105)\Gamma}\right] - \frac{1}{3}\left(\frac{\lambda_1}{\hbar}\right)^2\sum_k \alpha_1^2(k)\right.$$
$$\times\left\{\frac{2}{5}\,\frac{\omega_k+(2n_k+1)[\omega-\omega_M-60+(8/21)\Gamma]}{[\omega-\omega_M-60+(8/21)\Gamma]^2-\omega_k^2} + \frac{(2n_{k+1})(\omega-\bar{\omega}_M)}{(\omega-\omega_M)^2-\omega_k^2}\right\} - \frac{2}{5}\left(\frac{\lambda_2}{\hbar}\right)^2\sum_k \alpha_2^2(k)\left\{\frac{1}{9}\,\frac{\omega_k-(2n_k+1)[\omega-\bar{\omega}_M+40-(16/105)\Gamma]}{[\omega-\bar{\omega}_M+40-(16/105)\Gamma]^2-\omega_k^2}\right.$$
$$\left.\left.+\frac{3}{35}\,\frac{\omega_k+(2n_k+1)[\omega-\bar{\omega}_M-120-(16/45)\Gamma]}{[\omega-\bar{\omega}_M-120-(16/45)\Gamma]^2-\omega_k^2} + \frac{16}{45}\,\frac{\omega_k+(2n_k+1)[\omega-\bar{\omega}_M-20-(8/15)\Gamma]}{[\omega-\bar{\omega}_M-20-(8/15)\Gamma]^2-\omega_k^2}\right\}\right) = \frac{1}{2\pi}\left\{n_{00} + n_{10}\,\frac{1}{3}\left(\frac{\lambda_1}{\hbar}\right)^2\right.$$
$$\times\ \frac{2}{5}\,\frac{1}{\omega-\bar{\omega}_M-40+(16/105)\Gamma}\sum_k \alpha_1^2(k)\,\frac{\omega_k-(2n_k+1)[\omega-\bar{\omega}_M-60-(8/21)\Gamma]}{[\omega-\bar{\omega}_M-60-(8/21)\Gamma]^2-\omega_k^2}$$
$$\left.+\frac{1}{\omega-\omega_M+20+(8/15)\Gamma}\sum_k \alpha_1^2(k)\,\frac{(2n_k+1)(\omega-\bar{\omega}_M)}{(\omega-\bar{\omega}_M)^2-\omega_k^2} - \frac{2}{5}\,\frac{1}{\omega-\bar{\omega}_M-40+(16/105)\Gamma}\sum_k \alpha_1^2(k)\,\frac{\omega_k+(2n_k+1)(\omega-\bar{\omega}_M)}{(\omega-\bar{\omega}_M)^2-\omega_k^2}\right\}\ . \tag{46}$$

Furthermore, at low temperature the temperature dependence of the vibrational occupation number can be neglected and, accordingly, n_v for $v=0$ is one and for $v=1$, zero.

IV. RESULTS AND DISCUSSION

The infrared absorption coefficient is proportional to the imaginary part of $G(0,1)$, [Eq. (1)]

$$Q(\omega) \sim \omega\,\mathrm{Im}\,G(0,1)\ . \tag{47}$$

Since $G(0,1)$, as given by Eq. (46), is not written in a form that lends itself easily to analytical calculations, a program has been written to numerically determine its imaginary contribution and map the band shape. The linewidth (FWHM) is then directly determined from a plot of the line shape. As previously stated, four parameters are involved in the calculations: $V^{(2)}$, Λ_2, λ_1, and λ_2. Those that fit the experimental data have been chosen by a trial and error procedure and are given below. The number of significant figures given in each case is a measure of the uncertainty

$$V^{(2)} = 14\ \mathrm{cm}^{-1},\quad \Lambda_2 = 0.09\times10^3\ \mathrm{dyn/cm}\ ,$$
$$\lambda_1 = \pm 36.0\times10^{-7}\ \mathrm{dyn},\quad \lambda_2 = \pm 4.0\times10^{-7}\ \mathrm{dyn}\ . \tag{48}$$

The static barrier to rotation $V^{(2)}$ affects the position of the band center which shifts to higher frequencies as $V^{(2)}$ increases. Arguments based on a simple model have lead Schoen and co-workers[1] to estimate from the experimental data a value of 21.0 cm^{-1} for the height of this barrier for HCl in solid Ar which is consistent with what is calculated here. The force constant Λ_2

TABLE II. Calculated variation of linewidth $R(0)$, (FWHM), with temperature using parameters given in the text.

Temp. (K)	$\Delta\nu$ (cm^{-1})
5	0.9
10	1.05
15	1.40
20	1.85
25	2.50
30	3.35

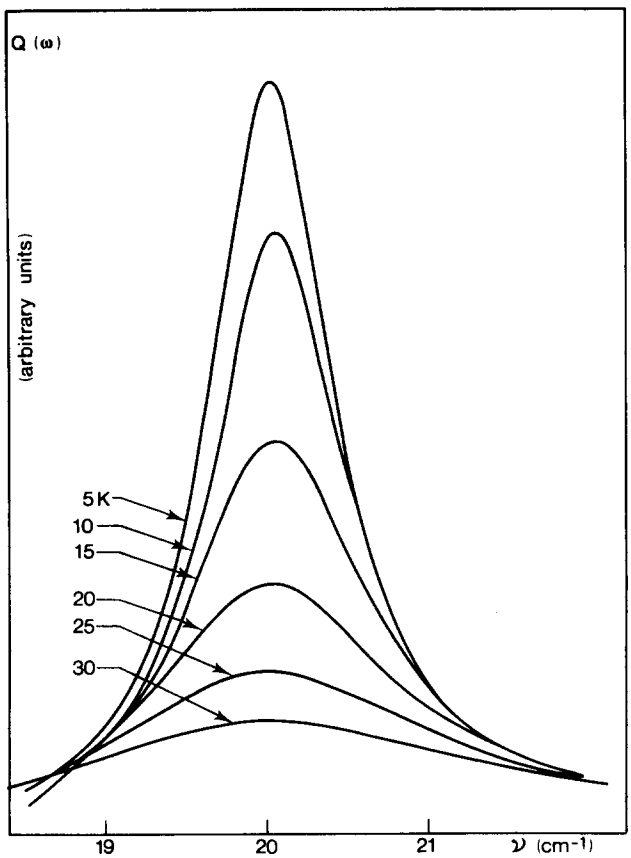

FIG. 4. Calculated band shape of the $R(0)$ line at various temperatures.

related to the binding of HCl in the Ar matrix, can be compared to the force constant associated to the bonding of two atoms in an Ar crystal namely 0.8×10^3 dyn/cm.[38] The much smaller value of Λ_2 suggests that the binding between the HCl impurity and its nearest neighbors is weaker than between adjacent Ar atoms of the unperturbed lattice. As for the parameters λ_1 and λ_2 they cannot be simply related to any physical quantity that can be easily extracted from the experimental data. It can only be stated that the experimental results are far more sensitive to changes in λ_1 than to λ_2. The results of the numerical calculations of the $R(0)$ band shape performed by varying ω between 18.5 and 22.5 cm^{-1} for a series of temperatures are plotted on Fig. 4. Values of the (FWHM) for each temperature are given in Table II and are also reported on Fig. 2 in order to compare experiment with theory. The agreement between observed and calculated (FWHM) is quite satisfactory within the entire temperature range. Furthermore, the changes in band shape with temperature are generally in accord with experiment although the ratios of the calculated intensities are probably exaggerated. A better fit to the observed data cannot be expected from the crude model adopted here. The present calculation only emphasizes that in the framework of this model the phonon coupling may be an efficient process in rotational line broadening. Work is actually in progress in order to extend the model to the case of a more realistic three-dimensional potential.

ACKNOWLEDGMENT

It is a pleasure for one of us (M. A.) to thank the laboratory for Research on the Structure of Matter (University of Pennsylvania) for making it possible to complete much of this work during June and July 1980.

APPENDIX

Coefficients appearing in the Hamiltonian operator [Eq. (20)]

$$A_1(l,m)=\left[\frac{(l+m+1)(l-m+1)}{(2l+1)(2l+3)}\right]^{1/2},$$

$$A_2(l,m)=A_1(l,m)A_1(l+1,m),$$

$$A_3(l,m)=2[A_1^2(l,m)+A_1^2(l-1,m)]-1,$$

$$\alpha_1(k)=-2\left(\frac{\hbar}{mN}\right)\omega_k^{-1/2}(1-\cos ka),$$

$$\alpha_2(k)=i2\left(\frac{\hbar}{mN}\right)\omega_k^{-1/2}\sin ka,$$

$$\beta_1(k,k')=-i2\left(\frac{\hbar}{mN}\right)(\omega_k\omega_{k'})^{-1/2}\times[\sin ka+\sin k'a-\sin(k+k')a],$$

$$\beta_2(k,k')=2\left(\frac{\hbar}{mN}\right)(\omega_k\omega_{k'})^{-1/2}\times[1-\cos ka-\cos k'a+\cos(k+k')a].$$

When necessary, the summations over k are performed within the framework of the harmonic approximation for the linear chain, i.e., $\omega_k=2\omega_L(1-\cos ka)$, with $\omega_L=(f/m)^{1/2}$ and the density of states is taken as

$$\rho(\omega_k)=\frac{2N}{\pi}\frac{1}{(\omega_L^2-\omega_k^2)^{1/2}}.$$

Thus,

$$N(T)=\sum_k\beta_2(k,-k)(n_k+\tfrac{1}{2})=\frac{16\hbar}{m\pi\omega_L}\int_0^{\pi/2}\frac{\sin\theta}{\exp(\beta\hbar\sin\theta)-1}d\theta.$$

[1] L. J. Schoen, D. E. Mann, C. Knobler, and D. White, J. Chem. Phys. **37**, 1146 (1962).
[2] D. E. Mann, L. J. Schoen, C. Knobler, and D. White, Proc. Int. Symp. Mol. Struct. Spectrosc. Tokyo A **209**, 1962 (1962).
[3] H. F. Shurvell, Ph. D. thesis, University of British Columbia, 1964: Diss. Abstr. **25**, 2260 (1964).
[4] D. E. Mann, N. Acquista, and D. White, J. Chem. Phys. **44**, 3453 (1966).
[5] J. M. P. J. Verstegen, H. Goldring, S. Kimel, and B. Katz, J. Chem. Phys. **44**, 3216 (1966).
[6] M. T. Bowers and W. H. Flygare, J. Mol. Spectrosc. **19**, 325 (1966).
[7] M. T. Bowers and W. H. Flygare, J. Chem. Phys. **44**, 1389 (1966).
[8] L. F. Keyser and G. W. Robinson, J. Chem. Phys. **44**, 3225 (1966).
[9] L. F. Keyser and G. W. Robinson, J. Chem. Phys. **45**, 1694 (1966).
[10] B. Katz, A. Ron, and O. Schnepp, J. Chem. Phys. **46**, 1926

(1967).
[11]K. B. Harvey and H. F. Shurvell, Chem. Commun. **1967**, 490.
[12]K. B. Harvey and H. F. Shurvell, Can. J. Chem. **45**, 2689 (1967).
[13]R. Ranganath, T. E. Whyte Jr., T. Theophanides, and G. C. Turrell, Spectrochim. Acta, Part A **23**, 807 (1967).
[14]A. J. Barnes, H. E. Hallam, and G. F. Scrimshaw, Trans. Faraday Soc. **65**, 3159 (1969).
[15]A. J. Barnes, J. B. Davies, H. E. Hallam, and G. F. Scrimshaw, Chem. Commun. **19**, 1089 (1969).
[16]W. G. Von Holle and D. W. Robinson, J. Chem. Phys. **53**, 3768 (1970).
[17]B. Katz and A. Ron, Chem. Phys. Lett. **7**, 357 (1970).
[18]J. B. Davies and H. E. Hallam, Trans. Faraday Soc. **67**, 3176 (1971).
[19]D. Maillard, A. Schriver, J. P. Perchard, C. Girarded, and D. Robert, J. Chem. Phys. **67**, 3917 (1977).
[20]J. M. Wiesenfeld and C. B. Moore, J. Chem. Phys. **70**, 930 (1979).
[21]L. Pauling, Phys. Rev. **36**, 430 (1930).
[22]A. F. Devonshire, Proc. R. Soc. London, Ser. A **153**, 601 (1936).
[23]H. Friedmann and S. Kimel, J. Chem. Phys. **43**, 3925 (1965).
[24]H. Friedmann and S. Kimel, J. Chem. Phys. **41**, 2552 (1964).
[25]H. Friedmann and S. Kimel, J. Chem. Phys. **44**, 4359 (1966).
[26]H. Friedmann and S. Kimel, J. Chem. Phys. **47**, 3589 (1967).
[27]G. K. Pandey and S. Chandra, J. Chem. Phys. **45**, 4369 (1966).
[28]P. O. Mannheim and H. Friedmann, Phys. Status Solidi **39**, 409 (1970).
[29]A. Nitzan and J. Jortner, Mol. Phys. **25**, 713 (1973).
[30]A. Nitzan, S. Mukamel, and J. Jortner, J. Chem. Phys. **63**, 200 (1975).
[31]F. Legay, *Chemical and Biological Application of Lasers*, edited by C. B. Moore (Academic, New York, 1978), p. 3.
[32]D. E. Mann, N. Acquista, and D. White, J. Chem. Phys. **44**, 3453 (1966).
[33]D. White and D. E. Mann, Rev. Sci. Instrum. **34**, 1370 (1963).
[34]K. N. Narahavi Rao and P. E. Fraley, Appl. Opt. **2**, 1127 (1963).
[35]E. Blaisten-Barojas and M. Allavena, Int. J. Quantum Chem. **8**, 195 (1973).
[36]E. Blaisten-Barojas and M. Allavena, J. Phys. C **9**, 3121 (1976).
[37]D. N. Zubarev, Sov. Phys. Usp. **3**, 320 (1960).
[38]G. L. Pollack, Rev. Mod. Phys. **36**, 748 (1964).